frontiers | Frontiers in Earth Science

ORIGINAL RESEARCH
published: 19 May 2022
doi: 10.3389/feart.2022.891032

Geochemical Composition of Surface Sediments in the Bashang Area, North China and its Environmental Significance

Linjing Liu[1,2], *Gaolei Jiang*[1,2]*, *Xin Mao*[1,2]*, *Hongmei Zhao*[1,2], *Yongjie Zhao*[3], *Yuecong Li*[3], *Hua Zhao*[1,2] *and Zhiwei Bi*[1,2]

[1]Institute of Hydrogeology and Environmental Geology, Chinese Academy of Geological Sciences, Shijiazhuang, China, [2]Key Laboratory of Quaternary Chronology and Hydrological Environment Evolution, China Geological Survey, Shijiazhuang, China, [3]College of Geographical Sciences, Hebei Normal University, Shijiazhuang, China

OPEN ACCESS

Edited by:
Zhiwei Xu,
Nanjing University, China

Reviewed by:
Mengying He,
Nanjing Normal University, China
Hongya Wang,
Peking University, China
Xusheng Li,
Nanjing University, China

***Correspondence:**
Gaolei Jiang
jianggl198899@163.com
Xin Mao
maoxin.iheg@cnu.edu.cn

Specialty section:
This article was submitted to Quaternary Science, Geomorphology and Paleoenvironment, a section of the journal Frontiers in Earth Science

Received: 07 March 2022
Accepted: 15 April 2022
Published: 19 May 2022

Citation:
Liu L, Jiang G, Mao X, Zhao H, Zhao Y, Li Y, Zhao H and Bi Z (2022) Geochemical Composition of Surface Sediments in the Bashang Area, North China and its Environmental Significance. Front. Earth Sci. 10:891032. doi: 10.3389/feart.2022.891032

The geochemical characteristics of sediments are important for reconstructing paleoclimatic and paleoenvironmental conditions in the Asian summer monsoon marginal area. However, robust reconstructions require an understanding of the key factors and mechanisms governing the spatial variations in the composition and ratio of chemical elements in the modern sediments of the Asian summer monsoon marginal area. In this study, 128 surface sediment samples were collected from the Bashang area, which is situated in the Asian summer monsoon marginal area, and examined for their major and trace element compositions and grain size. Principal component analysis (PCA) and redundancy analysis (RDA) were used to analyse the relationship between geochemical data and modern temperature and precipitation data. The results showed that the CIA values of sediments in the Bashang area are mainly affected by temperature rather than precipitation and the Rb/Sr value in the study area reflects the level of precipitation in the corresponding period and the temperature controlling the leaching and weathering. In addition, SiO_2/Al_2O_3 and Zr/Ti ratios have good positive relationships with the coarse-grained fraction of sediments and thus can be used as grain size proxies. We propose that the exact environmental significance indicated by these proxies should be stated explicitly before using them as proxies for paleoenvironmental reconstructions of the Asian summer monsoon marginal area.

Keywords: geochemistry, chemical index of alteration (CIA), rb/sr, SiO2/Al2O3, bashang area, environmental significance

1 INTRODUCTION

The geochemical characteristics of sediments can provide information on provenance and weathering, transport, and sedimentation processes (Wittkop et al., 2020; Yang et al., 2021). Thus, the geochemical characteristics of sediments can help determine the provenance of aeolian deposits, elucidate weathering processes, and further serve as proxies for reconstructing paleoclimatic and paleoenvironmental conditions (Zhao et al., 2019; Skurzyński et al., 2020). For example, the chemical index of alteration (CIA) is often used to evaluate the intensity of chemical weathering (Xiong et al., 2010; Buggle et al., 2011; Dinis et al., 2020), and the Rb/Sr ratios in loess-paleosol sequences can reveal the East Asian winter monsoon intensity (Chen et al., 1999; Jin et al., 2006). In addition, the SiO_2/Al_2O_3 ratio can be used as a grain size proxy (Hatano et al., 2019). Geochemical proxies are influenced by various factors, such as the mineral composition of parent rocks, changes in material sources and sedimentary processes (Borges et al., 2008; Garzanti et al., 2011; Wang et al., 2012; Shang et al., 2013; Hu and Yang, 2016; Peng et al., 2016; Chen et al., 2018; Guo et al., 2018; Li et al., 2019; Chen C. et al., 2021). Borges et al. (2008) found that the continuous cycle of sedimentation and the inheritance of the material from the previous sedimentary cycle greatly influence the application of chemical weathering indicators. Garzanti et al. (2011) suggested that hydraulics, such as suspension screening and selective entraining, greatly impact the elemental composition of sediments, and the CIA and other chemical weathering indicators lose their significance in indicating the degree of chemical weathering during hydraulic processes.

The East Asian summer monsoon (EASM) margin environment, defined as the semiarid zone in northern China, with mean annual precipitation ranging from 400 to 200 mm, is highly vulnerable to climate change (Jiang et al., 2020; Ming et al., 2021). In this region, widespread aeolian deposits, paleosols and lacustrine sediments have recorded a long history of changing environmental conditions under the influence of Asian monsoons (Yang and Ding, 2008; Zhen et al., 2021). Therefore, this region is a focus for historical reconstructions of monsoon changes (Xiao et al., 2006; Fan et al., 2017; Sun et al., 2018; Ding et al., 2019). Elemental compositions and ratios are commonly used reconstruction proxies (Liu B. et al., 2018; Liu J. et al., 2018; Chen Q. et al., 2021; Liu M. et al., 2021). However, robust reconstructions require an understanding of the key factors governing the spatial variations in the compositions and ratios of chemical elements in the modern sediments of the marginal Asian summer monsoon area.

The Bashang area, which connects the southeastern margin of the Inner Mongolia Plateau and the northern part of the Yan Mountains, northern China, is situated in the northeast Asian summer monsoon marginal area. The Asian monsoon margin is the most sensitive region to changes in monsoons. Specifically, environmental changes in northernmost margin of the EASM reflect the advance and retreat of the summer monsoon system and its interaction with the surrounding climate system (Gao et al., 2020). Moreover, this region is a representative agro-pastoral transitional zone and has a fragile ecological environment (Liu X. et al., 2021). Therefore, this region is ideal for studying the spatial variability of the composition and ratio of chemical elements in modern sediments, as well as its influential factors in the Asian summer monsoon marginal area. However, the spatial variability of chemical elements in modern sediments, as well as its influential factors in the Bashang area, remain uncertain.

In this study, 128 surface sediment samples were collected from the Bashang area and examined for their major and trace element contents and grain size. The objectives of this study were to investigate the mechanisms that control the spatial variability of chemical proxies in the surface sediments of the Asian summer monsoon marginal area, such as the CIA, Rb/Sr ratio, and SiO_2/Al_2O_3 ratio, which are commonly used indices for paleoenvironmental reconstruction, and to assess the potential for the use of those chemical proxies as indicators of environmental conditions.

2 STUDY AREA

The Bashang area is situated in the transition zone from the Inner Mongolia Plateau to the mountainous area in the northern mountains of Hebei Province (**Figure 1**). The area is surrounded by mountain ranges, such as the Yinshan Mountains to the north, the Yanshan Mountains to the south, and the Greater Khingan Range to the east (**Figure 1**). The Bashang area ranges from 1,350 m to 1,600 m in elevation, and the elevation decreases from south to north.

Climatologically, the Bashang area is located in the Asian summer monsoon marginal area and is characterized by a continental climate (Liu M. et al., 2021). The wind directions are dominated by northwest winds, which are driven by winter monsoonal winds from the Siberian high-pressure system. The mean annual temperature (MAT) values in this region range from 2 to 5°C, and they increase from east to west. Precipitation is mainly concentrated from July to September. The windy days and frost-free periods are 60–90 days and 80–100 days, respectively. The mean annual precipitation (MAP) gradually increases from 260 in the northwest to 400 mm in the southeast. Moreover, the mean annual potential evaporation values range from 1700 to 1800 mm, which are 4–5 times the MAP. The soil types are mainly chestnut soil and sandy soil. The soil textures are mainly sandy and clayey, and the soil layer is relatively thin (Wu and Zhao, 2017).

3 MATERIALS AND METHODS

3.1 Sample Collection

In this study, 128 surface sediment samples were collected from the Bashang area (**Figure 1A**). These samples were obtained mainly from areas that are less affected by human activities. The sediment types were mainly alluvial and lacustrine deposits. A representative 10 m × 10 m quadrat was selected, and then surface samples were collected from the top 1–2 cm at the four corners and centre of the quadrat according to the plum blossom point method. The lithology of the samples is mainly fine sand, with small amounts of medium sand and silt.

3.2 Sample Analysis

Approximately 5 g dried samples were ground to less than 200 mesh with an agate mortar and then pressed into tablets using the boric acid pressing method (Ji et al., 2003) at a high pressure of 30 tonnes. The concentrations of major elements and trace elements in our samples were determined by X-ray fluorescence (XRF) spectrometry (Panalytica) at Nanjing Normal University. The instrument used Hongze Lake Sediment GSS-9 (GBW07423) as a standard material for quality control. The analytical uncertainties (relative standard deviations) were less than 10%.

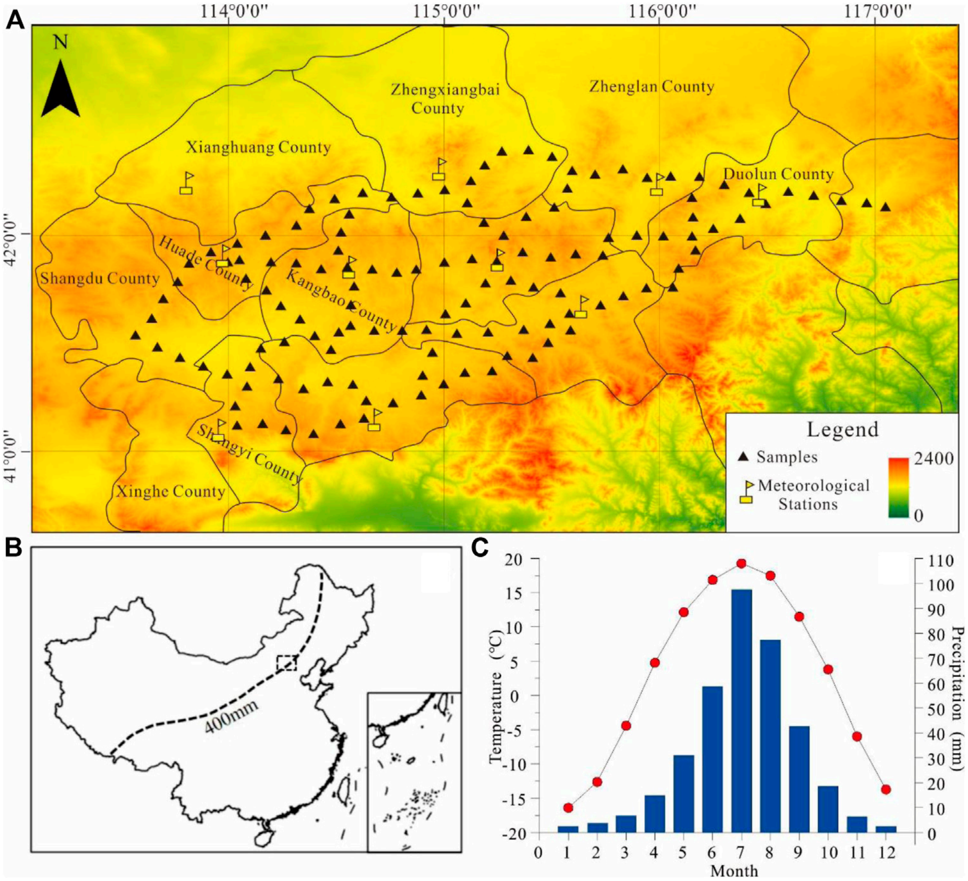

FIGURE 1 | (A) and **(B)** Location of the study area **(C)** Monthly mean temperatures and monthly mean precipitation values in the Bashang area.

TABLE 1 | Climatic conditions of the Bashang area, including the MAT and MAP, calculated based on meteorological data between 1960 and 2018 from ten meteorological stations in the Bashang area obtained from the China Meteorological Data Sharing Service System.

Meteorological Station	Longitude	Latitude	Annual Average Temperature (MAT; °C) (°C)	Annual Precipitation (MAP; mm)
Xianghuang County	113.8333	42.2333	3.7	262.9
Zhengxiangbai County	115.0000	42.3000	2.5	351.3
Zhenglan County	116.0000	42.2333	2.3	364.1
Duolun County	116.4667	42.1833	2.5	376.0
Taipusi County	115.2667	41.8833	2.1	393.4
Huade County	114.0000	41.9000	2.9	320.2
Kangbao County	114.5833	41.8500	1.9	347.6
Guyuan County	115.6500	41.6667	2.1	398.2
Shangyi County	113.9833	41.1000	3.8	415.7
Zhangbei County	114.7000	41.1500	3.4	387.6

The grain size of the samples was determined using a Malvern Mastersizer 2000 at the Key Laboratory of Quaternary Chronology and Hydrological Environment Evolution, China Geological Survey. This apparatus, with a measurement range of 0.02–2000 μm, was produced by Malvern Instruments Ltd., United Kingdom. Samples were first pretreated with 10% H_2O_2 and 30% HCl to remove organic matter and carbonates, respectively, and then dispersed by ultrasonication with 10 ml 10% boric acid solution. Then, the samples were analysed. Replicate analyses indicate that the mean particle size measurement error is <2%.

3.3 Meteorological Data

The MAT and MAP were calculated based on meteorological data between 1960 and 2018 from ten meteorological stations in the

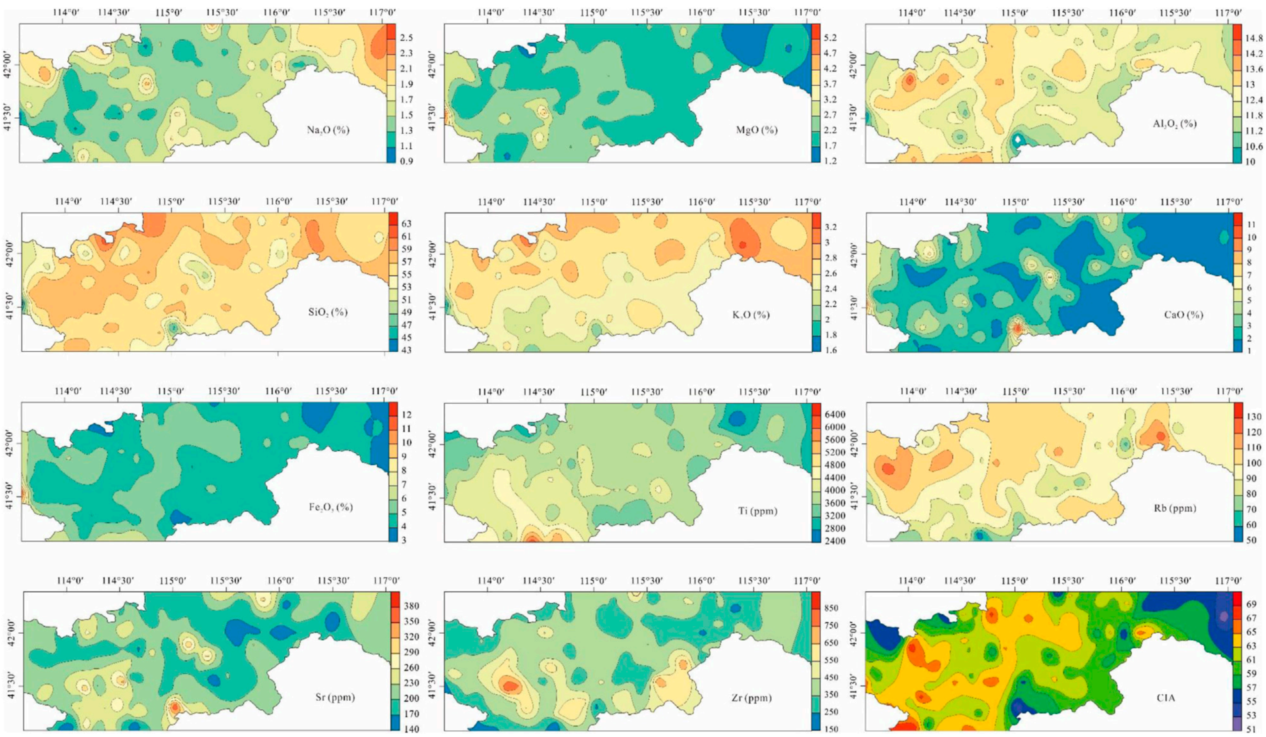

FIGURE 2 | Spatial distribution of elements in the surface sediments of the Bashang area.

Bashang area (**Table 1**). Then, the kriging model data interpolation method was used to obtain the MAT and MAP at each sampling point.

3.4 Data Analysis

Common element proxies, such as the CIA and Rb/Sr and SiO_2/Al_2O_3 ratios, were determined from the surface sediments of this study. The CIA (Nesbitt and Young, 1982) was calculated as follows:

$$CIA = Al_2O_3/(Al_2O_3 + K_2O + Na_2O + CaO^*) \times 100$$

where CaO^* refers to the amount of CaO incorporated in the silicate fraction of the samples, which was determined in our study following the method of McLennan (1993).

Principal component analysis (PCA) and redundancy analysis (RDA) were used for ordination of the geochemical data and the temperature, precipitation and mean grain size of the sediment samples. Log(x+1) transformations were applied before ordination analysis. Ordination analysis was used to explore the spatial distribution of element contents and the relation between the element contents and environmental variables. Log(x+1) transformations were applied before ordination analysis. Monte Carlo permutation tests (499 unrestricted permutations) were conducted to test the significance of variables, and forward selection was used to determine the minimum subset of significant variables. The ordinations were performed using the CANOCO program, version 5.0 (Šmilauer and Lepš, 2014).

4 RESULTS

4.1 Major and Trace Element Compositions

SiO_2 had the highest mean concentration of 56.28%, and the concentrations ranged from 43.36 to 62.92%. The concentrations of Al_2O_3 in the surface sediments ranged from 9.25 to 15.31%, with a mean concentration of 12.49%. The concentrations of Fe_2O_3 ranged from 3.07 to 11.99%, with a mean concentration of 4.89%. The K_2O, Na_2O, CaO, and MgO concentrations were 1.53% (0.94–2.56%), 2.63% (1.64–3.28%), 2.89% (1.23–12.36%), and 2.21% (1.26–5.31%), respectively. Among the trace elements, the mean concentrations of Rb, Sr, Ti and Zr in the surface sediments were 96.96 ppm (50.50–128.20 ppm), 210.71 ppm (137.00–400.90 ppm), 3892.90 ppm (2479.10–6506.80 ppm) and 387.88 ppm (190–840 ppm), respectively. The concentration of SiO_2 showed relatively small spatial variations within the Bashang area (**Figure 2**), while other major and trace elements showed considerable spatial variations. Higher concentrations of Al_2O_3 and Rb occurred in the western part of the Bashang area, while higher concentrations of both Zr and Ti were observed in the southern and western parts of the Bashang area (**Figure 2**).

The average CIA value was 61.59, and the values ranged from 51.17 to 69.34, while the average Rb/Sr value was 0.477, and the values ranged from 0.16 to 0.75. Higher CIA values occurred in the western part of the Bashang area, and Rb/Sr values were the highest in the northwestern part of the Bashang area (**Figure 2**).

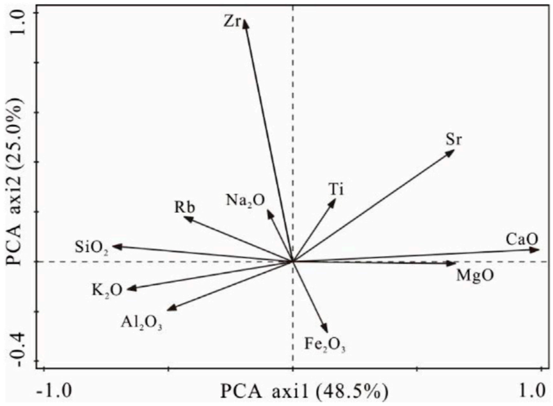

FIGURE 3 | PCA biplot of different elements in the surface sediments of the Bashang area.

The PCA results showed two principal components that accounted for 73.5% of the total variance (**Figure 3**). The first principal component (PC1) was positively correlated with MgO, CaO, and Sr and negatively correlated with SiO_2, K_2O, Al_2O_3 and Rb in the sediments (**Figure 3**). The second principal component (PC2) had high positive loadings of Zr and Ti and negative correlations with Fe_2O_3 (**Figure 3**). The RDA results showed that the first axis of the RDA captured 13% of the total variance, and the second axis captured 8%. The results showed one strong positive relationship between the CIA and Ti, temperature and clay content (**Figure 5**), and the arrows of the first axis were positioned in the negative direction. Zr and Si/Al and the fine and coarse sand contents had a positive relationship, and the arrows were positioned in the negative direction of the first axis. Rb/Sr had a weak relationship with the environmental parameters.

4.2 Grain Size

The grain size analysis revealed that the samples were dominated by fine sand (64–255 μm) and silt (4–63 μm). The mean contents of the clay (<4 μm), silt (4–63 μm), and fine sand (64–255 μm) fractions were 15.80, 44.36 and 28.30%, respectively. Moreover, the mean contents of the medium sand (256–512 μm) and coarse sand (512–2000 μm) fractions were relatively low.

The mean contents of the clay, silt and fine sand fractions showed relatively small spatial variations within the Bashang area (**Figure 4**). The mean contents of the medium and coarse sand fractions showed considerable spatial variations, and higher medium and coarse sand fractions were identified in the southwestern and northeastern parts of the Bashang area (**Figure 4**).

5 DISCUSSION

5.1 Proxy Interpretation

5.1.1 CIA

The CIA was first proposed by Nesbitt and Young (1982) to reconstruct the paleoclimate from the early Proterozoic sediments of the Huronian Supergroup, north of Lake Huron. The CIA has been widely used to quantitatively evaluate the chemical weathering intensity (Guo et al., 2018; Wang et al., 2020) and represents the ratio of mobile soluble elements (i.e., CaO, Na_2O, and K_2O) to immobile insoluble elements (i.e., Al_2O_3). Generally, higher CIA values indicate stronger chemical weathering (Xie et al., 2018; Chen C. et al., 2021). CIA values <50 indicate virtually no weathering; CIA values of approximately 50–60 indicate weak chemical weathering; and CIA values >80 indicate strong chemical weathering (Zhao et al., 2018).

Previous studies have suggested that climate, especially precipitation, exerts a dominant control on silicate weathering (White and Blum, 1995; Dinis et al., 2020). However, in this study, the RDA results show that the CIA exhibits better correlations with the MAT values and clay fractions and poorer correlations with the MAP values. The intensity of weathering at the Earth's surface largely depends on climate, and the weathering intensity is higher in warmer and more humid settings. Based on the Arrhenius equation, the mineral decomposition rate at the watershed scale increases as temperature increases, and the reaction rate can be doubled for each 10 °C increase (White and Blum, 1995; Dessert et al., 2003). The influence of temperature on the weathering rate is dependent on precipitation (White and Blum, 1995). In the study area, precipitation gradually decreased from east to west due to the weakening of the Asian monsoon. However, temperature increased from east to west. The increase in the CIA values from east to west (**Figure 2**) and the RDA result (**Figure 5**) indicate that the CIA values of sediments in the Bashang area are mainly affected by temperature rather than precipitation.

5.1.2 Rb/Sr Ratio

Rb and Sr usually exhibit different geochemical behaviours in sediments during the processes of weathering, denudation, and transport (Amorosi et al., 2021). In comparison to Sr, Rb is relatively insoluble and can be immobilized by adsorption onto clay minerals (Chen et al., 1999; Liu et al., 2014; An et al., 2018). Thus, the Rb/Sr ratio is often considered a good proxy for the chemical weathering intensity in lacustrine sediments (Jin et al., 2001), loess-paleosol sediments (Liang et al., 2013), and aeolian sediments (Liu et al., 2014). Previous studies of weathering crusts and loess-paleosol sediments have suggested that higher Rb/Sr values in the residual component indicate stronger chemical weathering. The higher chemical weathering intensity of lake sediments in catchments corresponds to the low Rb/Sr ratios of lake sediments resulting from more dissolved Sr in the basin (Jin and Zhang, 2002; Jin et al., 2006).

In this study, the RDA results show that the Rb/Sr ratio has a negative correlation with the MAT and MAP values. The studies of loess-paleosol sequences show that the Rb/Sr value of the residual component gradually increases with the strengthening of chemical weathering (Chen et al., 1999; Chen et al., 2001). Accordingly, the Rb/Sr value in lacustrine sediments decreases with increasing chemical weathering rate in the basin (Jin et al., 2001). Therefore, generally, in dry and cold climate environments, chemical weathering is weak and the Rb/Sr value of lacustrine sediments is high. Under warm and humid conditions, chemical weathering is strong and the Rb/Sr value of lacustrine sediments is low. On the other hand, the variation

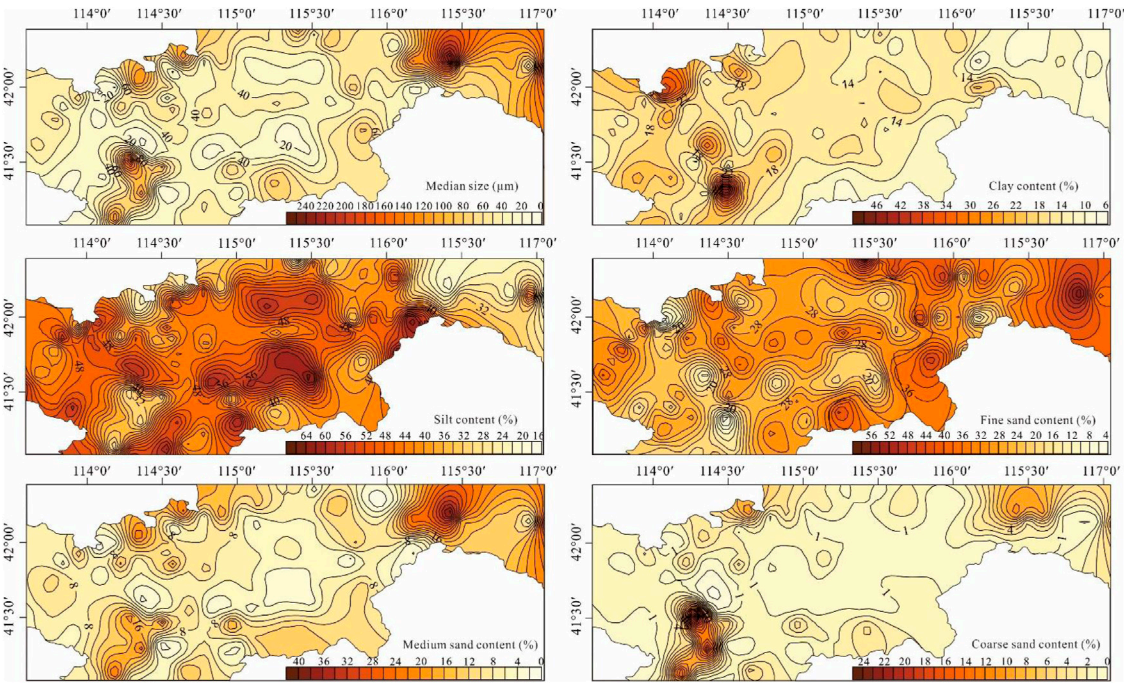

FIGURE 4 | Spatial distribution of grain size parameters.

range of Rb content in lacustrine sediments is very small, and the variation of Rb/Sr value mainly depends on the activity of Sr (Chen, et al., 1997). This is because the element Rb and Sr are easy to separate during rainwater leaching, Rb has a strong affinity with clay, and Sr easily enters the solution (Chen et al., 1997). Therefore, the Rb/Sr value in well preserved lacustrine sediments essentially indicates the degree of material leaching in the source area, and further reflects the level of precipitation in the corresponding period in the basin and the temperature controlling the leaching and weathering behavior.

5.1.3 SiO_2/Al_2O_3 Ratio

In general, coarse-grained sediments are enriched in quartz that has a high SiO_2 content. In contrast, fine-grained sediments usually tend to be enriched in micaceous and/or clay minerals that have high Al_2O_3 contents (Liang et al., 2013). Consequently, SiO_2/Al_2O_3 ratios are used as a grain size index (Hatano et al., 2019). In this study, the RDA results show that the mean and median grain sizes have significant positive correlations with the SiO_2/Al_2O_3 ratio. **Figure 6** also indicates that grain size exerts a strong influence on the SiO_2/Al_2O_3 ratio.

5.1.4 Ti and Zr Contents and Zr/Ti Ratio

Ti and Zr are presumably the least mobile elements during weathering and are mainly found in weathering-resistant silicate minerals, such as zircon and rutile, respectively (Dypvik and Harris, 2001; Kylander et al., 2013). Changes in the Ti and Zr contents can thus be used to qualitatively or semiquantitatively estimate detrital matter abundances

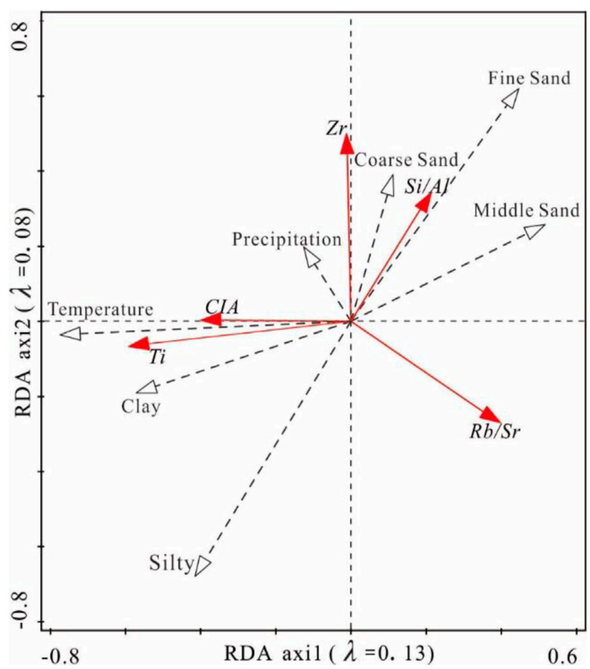

FIGURE 5 | RDA plot of environmental indices and factors.

(Francke et al., 2020). When the regional precipitation increases, large Ti and Zr abundances are brought into the lake during heavy runoff and heavy precipitation, and vice

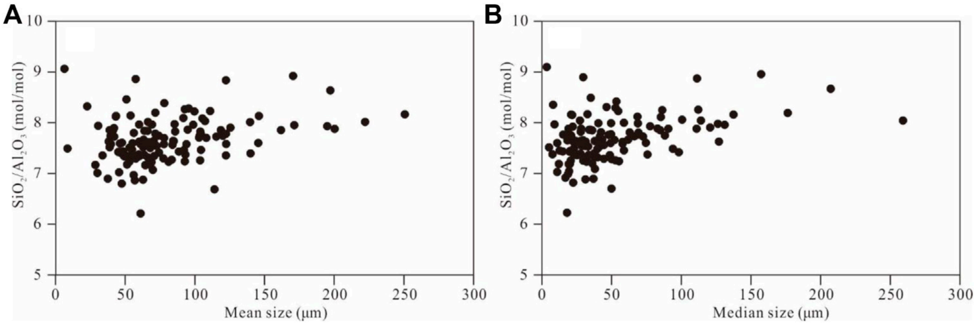

FIGURE 6 | Relationship between the SiO_2/Al_2O_3 ratio and the mean grain size **(A)** and median grain size **(B)** of sediments.

versa. Therefore, the Ti contents indicate the amounts of detrital sediments brought into the lake by regional precipitation or surface runoff to a certain extent (Shen et al., 2010; Biskaborn et al., 2012). In this study, the RDA results show that Zr exhibits a good correlation with the sand fraction, while Ti is associated with the clay and silt fractions. Thus, increases in the Zr/Ti ratio may be indicative of less clay and silt or more sand and can be used as a proxy for alterations in silicate sources.

5.2 Implications for Paleoenvironmental Reconstruction

As common geochemical proxies, the CIA, Rb/Sr ratio, SiO_2/Al_2O_3 ratio, and Zr/Ti ratio are widely used to assess various sediments (Roy et al., 2013; Francke et al., 2020). The CIA and Rb/Sr ratio are often used to evaluate the chemical weathering intensity (Garzanti et al., 2018). In this study, the CIA values have a good correlation with the clay components of sediments and temperature. The study area is located at the margin of the Asian monsoon, and the precipitation in this area is affected by the advance and retreat of the monsoon. The RDA results indicate that the CIA values of sediments in the Bashang area are mainly affected by temperature rather than precipitation. In the study area, the mean annual precipitation (MAP) gradually increases from 260 in the northwest to 400 mm in the southeast. It is possible that the changes in precipitation have a limited effect on the regional CIA. The Rb/Sr ratio has a negative correlation with the MAT and MAP values. The Rb/Sr ratio is affected by complex factors. Especially for the lacustrine sediments, the source of sediments has a great influence on Rb/Sr ratio (An et al., 2018). These negative correlations suggested that the Rb/Sr value in well preserved lacustrine sediments in the study area reflects the level of precipitation in the corresponding period in the basin and the temperature controlling the leaching and weathering behavior. The negative correlation between Rb/Sr ration and CIA value also indicates this point. The PCA results show that PC1 is positively correlated with MgO, CaO and Sr, which are easily transported elements, and is negatively correlated with SiO_2, K_2O, Al_2O_3 and Rb in the sediments, which are not easily transported (**Figure 3**). PC1 accounts for 48.5% of the total variance. Therefore, the changes in PC1 can be used as a comprehensive proxy of paleoclimate change.

Many studies have suggested that SiO_2/Al_2O_3 and Zr/Ti ratios can be used as grain size indices for aeolian sands (Chen Q. et al., 2021) and lake sediments (Kylander et al., 2013) in semiarid and arid regions. Our findings are consistent with these conclusions. The SiO_2/Al_2O_3 and Zr/Ti ratios in this study have a good positive relationship with the coarse-grained fraction of sediments and thus can be used as proxies for grain size.

6 CONCLUSION

The CIA values of sediments in the Bashang area are mainly affected by temperature. The Rb/Sr value in well preserved lacustrine sediments in the study area reflects the level of precipitation in the corresponding period in the source area and the temperature controlling the leaching and weathering behavior. Therefore, different geochemical proxies in the same sediments have different interpretation. The exact environmental significance indicated by these proxies should be stated explicitly before using them as proxies for paleoenvironmental reconstructions of the Asian summer monsoon marginal area. Statistical analyses of chemical changes may be able to identify more appropriate climate change proxies.

The mean and median grain sizes have significant positive correlations with the SiO_2/Al_2O_3 ratio. The SiO_2/Al_2O_3 ratio can therefore be used as a grain size index. Zr exhibits a good correlation with the sand fraction, while Ti is associated with the clay and silt fractions. Thus, the Zr/Ti ratio can be used as a proxy for alterations in silicate sources.

DATA AVAILABILITY STATEMENT

The original contributions presented in the study are included in the article/**Supplementary Material**, further inquiries can be directed to the corresponding authors.

AUTHOR CONTRIBUTIONS

All authors listed have made substantial, direct, and intellectual contributions to the work and have approved it for publication.

FUNDING

This research was financially supported by the National Natural Science Foundation of China (42177428, 41807420, 41907375, U20A20116, and 41602194) and the Basic Research Programme of the Institute of Hydrogeology and Environmental Geology, Chinese Academy of Geological Sciences (CAGS) (SK202007).

ACKNOWLEDGMENTS

We are grateful to Jiayi Xiao at Nanjing Normal University and other colleagues at the Institute of Hydrogeology and Environmental Geology, CAGS, who contributed to our field work and data analysis.

SUPPLEMENTARY MATERIAL

The Supplementary Material for this article can be found online at: https://www.frontiersin.org/articles/10.3389/feart.2022.891032/full#supplementary-material

REFERENCES

Amorosi, A., Bruno, L., Campo, B., Di Martino, A., and Sammartino, I. (2021). Patterns of Geochemical Variability across Weakly Developed Paleosol Profiles and Their Role as Regional Stratigraphic Markers (Upper Pleistocene, Po Plain). *Palaeogeogr. Palaeoclimatol. Palaeoecol.* 574, 110413. doi:10.1016/j.palaeo.2021.110413

An, F., Lai, Z., Liu, X., Fan, Q., and Wei, H. (2018). Abnormal Rb/Sr Ratio in Lacustrine Sediments of Qaidam Basin, NE Qinghai-Tibetan Plateau: A Significant Role of Aeolian Dust Input. *Quat. Int.* 469, 44–57. doi:10.1016/j.quaint.2016.12.050

Biskaborn, B. K., Herzschuh, U., Bolshiyanov, D., Savelieva, L., and Diekmann, B. (2012). Environmental Variability in Northeastern Siberia during the Last ~ 13,300 Yr Inferred from Lake Diatoms and Sediment-Geochemical Parameters. *Palaeogeogr. Palaeoclimatol. Palaeoecol.* 329-330, 22–36. doi:10.1016/j.palaeo.2012.02.003

Borges, J. B., Huh, Y., Moon, S., and Noh, H. (2008). Provenance and Weathering Control on River Bed Sediments of the Eastern Tibetan Plateau and the Russian Far East. *Chem. Geol.* 254, 52–72. doi:10.1016/j.chemgeo.2008.06.002

Buggle, B., Glaser, B., Hambach, U., Gerasimenko, N., and Marković, S. (2011). An Evaluation of Geochemical Weathering Indices in Loess-Paleosol Studies. *Quat. Int.* 240, 12–21. doi:10.1016/j.quaint.2010.07.019

Chen, C., Tao, S., Zhao, W., Jin, M., Wang, Z., Li, H., et al. (2021). Holocene Lake Level, Vegetation, and Climate at the East Asian Summer Monsoon Margin: A Record from the Lake Wulanhushao Basin, Southern Inner Mongolia. *Palaeogeogr. Palaeoclimatol. Palaeoecol.* 561, 110051. doi:10.1016/j.palaeo.2020.110051

Chen, J., An, Z., and Head, J. (1999). Variation of Rb/Sr Ratios in the Loess-Paleosol Sequences of Central China during the Last 130,000 Years and Their Implications for Monsoon Paleoclimatology. *Quat. Res.* 51, 215–219. doi:10.1006/qres.1999.2038

Chen, J., An, Z., Liu, L., Ji, J., Yang, J., and Chen, Y. (2001). Variations in Chemical Compositions of the Eolian Dust in Chinese Loess Plateau over the Past 2.5 Ma and Chemical Weathering in the Asian Inland. *Sci. China Ser. D-Earth Sci.* 44 (5), 403–413. doi:10.1007/bf02909779

Chen, J., Qiu, G., Lu, H., and Ji, J. (1997). Variation of Summer Monsoon Intensity on the Loess Plateau of Central China during the Last 130 000 a. *Chin. Sci. Bull.* 42, 473–476. doi:10.1007/bf02882595

Chen, Q., Li, Z., Dong, S., Wang, N. a., Lai, D. Y. F., and Ning, K. (2018). Spatial Variations in the Chemical Composition of Eolian Sediments in Hyperarid Regions: a Case Study from the Badain Jaran Desert, Northwestern China. *J. Sediment. Res.* 88, 290–300. doi:10.2110/jsr.2018.11

Chen, Q., Li, Z., Dong, S., Yu, Q., Zhang, C., and Yu, X. (2021). Applicability of Chemical Weathering Indices of Eolian Sands from the Deserts in Northern China. *CATENA* 198, 105032. doi:10.1016/j.catena.2020.105032

Dessert, C., Dupré, B., Gaillardet, J., François, L. M., and Allègre, C. J. (2003). Basalt Weathering Laws and the Impact of Basalt Weathering on the Global Carbon Cycle. *Chem. Geol.* 202, 257–273. doi:10.1016/j.chemgeo.2002.10.001

Ding, Z., Lu, R., Lyu, Z., and Liu, X. (2019). Geochemical Characteristics of Holocene Aeolian Deposits East of Qinghai Lake, China, and Their Paleoclimatic Implications. *Sci. Total Environ.* 692, 917–929. doi:10.1016/j.scitotenv.2019.07.099

Dinis, P. A., Garzanti, E., Hahn, A., Vermeesch, P., and Cabral-Pinto, M. (2020). Weathering Indices as Climate Proxies. A Step Forward Based on Congo and SW African River Muds. *Earth-Science Rev.* 201, 103039. doi:10.1016/j.earscirev.2019.103039

Dypvik, H., and Harris, N. B. (2001). Geochemical Facies Analysis of Fine-Grained Siliciclastics Using Th/U, Zr/Rb and (Zr+Rb)/Sr Ratios. *Chem. Geol.* 181, 131–146. doi:10.1016/S0009-2541(01)00278-9

Fan, J., Xiao, J., Wen, R., Zhang, S., Wang, X., Cui, L., et al. (2017). Carbon and Nitrogen Signatures of Sedimentary Organic Matter from Dali Lake in Inner Mongolia: Implications for Holocene Hydrological and Ecological Variations in the East Asian Summer Monsoon Margin. *Quat. Int.* 452, 65–78. doi:10.1016/j.quaint.2016.09.050

Francke, A., Holtvoeth, J., Codilean, A. T., Lacey, J. H., Bayon, G., and Dosseto, A. (2020). Geochemical Methods to Infer Landscape Response to Quaternary Climate Change and Land Use in Depositional Archives: a Review. *Earth-Science Rev.* 207, 103218. doi:10.1016/j.earscirev.2020.103218

Gao, Y. H., Li, Z. L., Zhu, R. X., and Wang, N. A. (2020). Quantitative Reconstruction of Holocene Millennial-Scale Precipitation in the Asian Monsoon Margin of Northwest China, Revealed by Phytolith Assemblages from Calcareous Root Tubes in the Tengger Desert. *Clim. Dyn.* 55 (3), 755–770. doi:10.1007/s00382-020-05293-4

Garzanti, E., Andó, S., France-Lanord, C., Censi, P., Vignola, P., Galy, V., et al. (2011). Mineralogical and Chemical Variability of Fluvial Sediments 2. Suspended-Load Silt (Ganga-Brahmaputra, Bangladesh). *Earth Planet. Sci. Lett.* 302, 107–120. doi:10.1016/j.epsl.2010.11.043

Garzanti, E., Dinis, P., Vermeesch, P., Andò, S., Hahn, A., Huvi, J., et al. (2018). Dynamic Uplift, Recycling, and Climate Control on the Petrology of Passive-Margin Sand (Angola). *Sediment. Geol.* 375, 86–104. doi:10.1016/j.sedgeo.2017.12.009

Guo, Y., Yang, S., Su, N., Li, C., Yin, P., and Wang, Z. (2018). Revisiting the Effects of Hydrodynamic Sorting and Sedimentary Recycling on Chemical Weathering Indices. *Geochimica Cosmochimica Acta* 227, 48–63. doi:10.1016/j.gca.2018.02.015

Hatano, N., Yoshida, K., Adachi, Y., and Sasao, E. (2019). Intense Chemical Weathering in Southwest Japan during the Pliocene Warm Period. *J. Asian Earth Sci.* 184, 103971. doi:10.1016/j.jseaes.2019.103971

Hu, F., and Yang, X. (2016). Geochemical and Geomorphological Evidence for the Provenance of Aeolian Deposits in the Badain Jaran Desert, Northwestern China. *Quat. Sci. Rev.* 131, 179–192. doi:10.1016/j.quascirev.2015.10.039

Jiang, M., Han, Z., Li, X., Wang, Y., Stevens, T., Cheng, J., et al. (2020). Beach Ridges of Dali Lake in Inner Mongolia Reveal Precipitation Variation during the Holocene. *J. Quat. Sci.* 35, 716–725. doi:10.1002/jqs.3195

Jin, Z., Cao, J., Wu, J., and Wang, S. (2006). A Rb/Sr Record of Catchment Weathering Response to Holocene Climate Change in Inner Mongolia. *Earth Surf. Process. Landforms* 31, 285–291. doi:10.1002/esp.1243

Jin, Z., Wang, S., Shen, J., Zhang, E., Li, F., Ji, J., et al. (2001). Chemical Weathering since the Little Ice Age Recorded in Lake Sediments: a High-Resolution Proxy of Past Climate. *Earth Surf. Process. Landforms* 26, 775–782. doi:10.1002/esp.224

Jin, Z., and Zhang, E. (2002). Paleoclimate Implications of Rb/Sr Ratios from Lake Sediments. *Sci. Technol. Eng.* 2, 20–22. CNKI:SUN:KXJS.0.2002-03-008

Kylander, M. E., Klaminder, J., Wohlfarth, B., and Löwemark, L. (2013). Geochemical Responses to Paleoclimatic Changes in Southern Sweden since the Late Glacial: the Hässeldala Port Lake Sediment Record. *J. Paleolimnol.* 50, 57–70. doi:10.1007/s10933-013-9704-z

Li, Z., Chen, Q., Zhang, C., Yu, Q., Dong, S., Zhao, L., et al. (2019). Environmental Significance of the Chemical Composition of Sediments in Groundwater-Recharged Lakes of the Badain Jaran Desert, NW China. *Geochem. Geophys. Geosyst.* 20, 1026–1040. doi:10.1029/2018GC007967

Liang, L., Sun, Y., Beets, C. J., Prins, M. A., Wu, F., and Vandenberghe, J. (2013). Impacts of Grain Size Sorting and Chemical Weathering on the Geochemistry of Jingyuan Loess in the Northwestern Chinese Loess Plateau. *J. Asian Earth Sci.* 69, 177–184. doi:10.1016/j.jseaes.2012.12.015

Liu, B., Jin, H., Sun, L., Niu, Q., Zhang, C., Xue, W., et al. (2018). Multiproxy Records of Holocene Millennial-Scale Climatic Variations from the Aeolian Deposit in Eastern Horqin Dune Field, Northeastern China. *Geol. J.* 54, 351–363. doi:10.1002/gj.3184

Liu, B., Jin, H., Sun, L., Sun, Z., Niu, Q., Xie, S., et al. (2014). Holocene Moisture Change Revealed by the Rb/Sr Ratio of Aeolian Deposits in the Southeastern Mu Us Desert, China. *Aeolian Res.* 13, 109–119. doi:10.1016/j.aeolia.2014.03.006

Liu, J., Wang, Y., Wang, Y., Guan, Y., Dong, J., and Li, T. (2018). A Multi-Proxy Record of Environmental Changes during the Holocene from the Haolaihure Paleolake Sediments, Inner Mongolia. *Quat. Int.* 479, 148–159. doi:10.1016/j.quaint.2016.12.015

Liu, M., Min, L., Zhao, J., Shen, Y., Pei, H., Zhang, H., et al. (2021). The Impact of Land Use Change on Water-Related Ecosystem Services in the Bashang Area of Hebei Province, China. *Sustainability* 13, 716. doi:10.3390/su13020716

Liu, X., Lu, R., Ding, Z., Lyu, Z., Li, Y., and Dong, Z. (2021). Holocene Environmental Changes Inferred from an Aeolian-Palaeosol-Lacustrine Profile in the Mu Us Desert, Northern China. *Front. Earth Sci.* 9, 799935. doi:10.3389/feart.2021.799935

McLennan, S. M. (1993). Weathering and Global Denudation. *J. Geol.* 101, 295–303. doi:10.1086/648222

Ming, G., Zhou, W., Wang, H., Shu, P., Cheng, P., Liu, T., et al. (2021). Grain Size Variation in Two Lakes from Margin of Asian Summer Monsoon and its Paleoclimate Implications. *Palaeogeogr. Palaeoclimatol. Palaeoecol.* 567, 110295. doi:10.1016/j.palaeo.2021.110295

Nesbitt, H. W., and Young, G. M. (1982). Early Proterozoic Climates and Plate Motions Inferred from Major Element Chemistry of Lutites. *Nature* 299, 715–717. doi:10.1038/299715a0

Peng, S., Hao, Q., Wang, L., Ding, M., Zhang, W., Wang, Y., et al. (2016). Geochemical and Grain-Size Evidence for the Provenance of Loess Deposits in the Central Shandong Mountains Region, Northern China. *Quat. Res.* 85, 290–298. doi:10.1016/j.yqres.2016.01.005

Roy, P. D., Quiroz-Jiménez, J. D., Pérez-Cruz, L. L., Lozano-García, S., Metcalfe, S. E., Lozano-Santacruz, R., et al. (2013). Late Quaternary Paleohydrological Conditions in the Drylands of Northern Mexico: a Summer Precipitation Proxy Record of the Last 80 Cal Ka BP. *Quat. Sci. Rev.* 78, 342–354. doi:10.1016/j.quascirev.2012.11.020

Shen, H. Y., Jia, Y. L., and Guo, F. (2010). Characteristics and Environmental Significance of the Magnetic Susceptibility in Sediment of Huangqihai Lake, Inner Mongolia, China. *Arid. Land Geogr.* 33, 151–157. doi:10.13826/j.cnki.cn65-1103/x.2010.02.002

Skurzyński, J., Jary, Z., Kenis, P., Kubik, R., Moska, P., Raczyk, J., et al. (2020). Geochemistry and Mineralogy of the Late Pleistocene Loess-Palaeosol Sequence in Złota (Near Sandomierz, Poland): Implications for Weathering, Sedimentary Recycling and Provenance. *Geoderma* 375, 114459. doi:10.1016/j.geoderma.2020.114459

Šmilauer, P., and Lepš, J. (2014). *Multivariate Analysis of Ecological Data Using CANOCO 5*. Cambridge, UK: Cambridge University Press.

Sun, Q., Chu, G., Xie, M., Zhu, Q., Su, Y., and Wang, X. (2018). An Oxygen Isotope Record from Lake Xiarinur in Inner Mongolia since the Last Deglaciation and its Implication for Tropical Monsoon Change. *Glob. Planet. Change* 163, 109–117. doi:10.1016/j.gloplacha.2018.01.017

Wang, P., Du, Y., Yu, W., Algeo, T. J., Zhou, Q., Xu, Y., et al. (2020). The Chemical Index of Alteration (CIA) as a Proxy for Climate Change during Glacial-Interglacial Transitions in Earth History. *Earth-Science Rev.* 201, 103032. doi:10.1016/j.earscirev.2019.103032

Wang, X., Xia, D., Zhang, C., Lang, L., Hua, T., and Zhao, S. (2012). Geochemical and Magnetic Characteristics of Fine-Grained Surface Sediments in Potential Dust Source Areas: Implications for Tracing the Provenance of Aeolian Deposits and Associated Palaeoclimatic Change in East Asia. *Palaeogeogr. Palaeoclimatol. Palaeoecol.* 323-325, 123–132. doi:10.1016/j.palaeo.2012.02.005

White, A. F., and Blum, A. E. (1995). Effects of Climate on Chemical_ Weathering in Watersheds. *Geochimica Cosmochimica Acta* 59, 1729–1747. doi:10.1016/0016-7037(95)00078-E

Wittkop, C., Bartley, J. K., Krueger, R., Bouvier, A., Georg, R. B., Knaeble, A. R., et al. (2020). Influence of Provenance and Transport Process on the Geochemistry and Radiogenic (Hf, Nd, and Sr) Isotopic Composition of Pleistocene Glacial Sediments, Minnesota, USA. *Chem. Geol.* 532, 119390. doi:10.1016/j.chemgeo.2019.119390

Wu, A. B., and Zhao, Y. X. (2017). Analysis of Ecological Land Pattern Evolution and Ecosystem Service Value in Bashang Plateau. *Trans. Chin. Soc. Agric. Eng.* 33 (2), 283–290.

Xiao, J., Wu, J., Si, B., Liang, W., Nakamura, T., Liu, B., et al. (2006). Holocene Climate Changes in the Monsoon/arid Transition Reflected by Carbon Concentration in Daihai Lake of Inner Mongolia. *Holocene* 16, 551–560. doi:10.1191/0959683606hl950rp

Xie, Y., Yuan, F., Zhan, T., Kang, C., and Chi, Y. (2018). Geochemical and Isotopic Characteristics of Sediments for the Hulun Buir Sandy Land, Northeast China: Implication for Weathering, Recycling and Dust Provenance. *CATENA* 160, 170–184. doi:10.1016/j.catena.2017.09.008

Xiong, S., Ding, Z., Zhu, Y., Zhou, R., and Lu, H. (2010). A ~6Ma Chemical Weathering History, the Grain Size Dependence of Chemical Weathering Intensity, and its Implications for Provenance Change of the Chinese Loess-Red Clay Deposit. *Quat. Sci. Rev.* 29, 1911–1922. doi:10.1016/j.quascirev.2010.04.009

Yang, S., and Ding, Z. (2008). Advance-retreat History of the East-Asian Summer Monsoon Rainfall Belt over Northern China during the Last Two Glacial-Interglacial Cycles. *Earth Planet. Sci. Lett.* 274, 499–510. doi:10.1016/j.epsl.2008.08.001

Yang, S., Luo, Y., Li, Q., Liu, W., Chen, Z., Liu, L., et al. (2021). Comparisons of Topsoil Geochemical Elements from Northwest China and Eastern Tibetan Plateau Identify the Plateau Interior as Tibetan Dust Source. *Sci. Total Environ.* 798, 149240. doi:10.1016/j.scitotenv.2021.149240

Yuan, S., Rui-Jie, L., Fei-Fei, J., Li-Hui, T., Qing-Liang, T., Yuan, C., et al. (2013). Paleoclimatic Evolution Indicated by Major Geochemical Elements from Aeolian Sediments on the East of Qinghai Lake. *Sci. Cold Arid Regions* 5, 301–308. doi:10.3724/SP.J.1226.2013.00301

Zhao, W., Liu, L., Chen, J., and Ji, J. (2019). Geochemical Characterization of Major Elements in Desert Sediments and Implications for the Chinese Loess Source. *Sci. China Earth Sci.* 62, 1428–1440. doi:10.1007/s11430-018-9354-y

Zhao, Z., Wen, X., Tang, L., Li, B., Niu, D., Meng, J., et al. (2018). Applicability of Chemical Alteration Index to Indication of Paleoclimate Change by Different Sedimentary Facies. *Acta Sedimentol. Sin.* 36, 343–353. doi:10.14027/j.issn.1000-0550.2018.026

Zhen, Z., Li, W., Xu, L., Zhang, X., and Zhang, J. (2021). Lake-level Variation of Dali Lake in Mid-east of Inner Mongolia since the Late Holocene. *Quat. Int.* 583, 62–69. doi:10.1016/j.quaint.2021.03.003

Conflict of Interest: The authors declare that the research was conducted in the absence of any commercial or financial relationships that could be construed as a potential conflict of interest.

Publisher's Note: All claims expressed in this article are solely those of the authors and do not necessarily represent those of their affiliated organizations, or those of the publisher, the editors and the reviewers. Any product that may be evaluated in this article, or claim that may be made by its manufacturer, is not guaranteed or endorsed by the publisher.

Copyright © 2022 Liu, Jiang, Mao, Zhao, Zhao, Li, Zhao and Bi. This is an open-access article distributed under the terms of the Creative Commons Attribution License (CC BY). The use, distribution or reproduction in other forums is permitted, provided the original author(s) and the copyright owner(s) are credited and that the original publication in this journal is cited, in accordance with accepted academic